Operating scenario of 3GWth class FFHR power plant with bypass controlled supercritical CO2 gas turbine power generation system

Operating scenario of 3GW$_{th}$Class FFHR power plant with bypass controlled supercritical CO_2 gas turbine power generation system

S.Ishiyama[*1], H.Chikaraishi[*2] and A.Sagara[*2]

[*1]*Faculty of Science and Technology, Graduate school of science and technology, Hirosaki University, Bunkyo1, Hirosaki, Aomori, Japan*

[*2] *National Institute for Fusion Science, Shimoishi 322-6 Toki, Gifu*

In order to achieve high power generation efficiency, facility compactness, high safety, and high coexistence with fuel tritium in the 3GW$_{th}$ class FFHR(Free Force Helical Reactor) power plant, optimization, performance and operation scenario of the power generation system of the power plant model using the axial flow type uniaxial supercritical CO_2 gas turbine power generation system were examined. As a result, the following conclusions were obtained.

(1) The most efficient and compact axial flow uniaxial design supercritical CO_2 gas turbine power generation system suitable for 3GW$_{th}$FFHR power plant has a maximum heat capacity of 1.5GW$_{th}$×2, and the gas turbine conversion rate at that time was evaluated as 46.38%(=1,252MWe/2,700MW$_{th}$). Therefore, split connection with two power generation systems is optimal for a 3GW$_{th}$ class FFHR power plant. Here, the operating speed of the turbo equipment was set to 3,600 rpm in order to adapt this plant model to the power supply system in Japan.

(2) Simultaneous supply of 818MWe/300sec electricity and 300MW$_{th}$/30days heat is required at startup of the FFHR.

(3) The in-house power during steady operation under the self-ignition condition was reduced to about 32.7MWe, and the amount of power generated at the transmission end was evaluated as 1,219MWe (= 1,219MW$_e$/3,000MW$_{th}$(total efficiency 40.6%)),

Key words: Super critical CO_2 gas turbine, Free Force Helical Reactor (FFHR), 3GW$_{th}$ plant, Start-up scenario, Bypass control, Axial-flow single-shaft design turbine, Self-ignition

1. Introduction

Fusion power plants have a high demand for internal power to drive the main body. Therefore, when operating the power plant, extremely high Q value (20 to 30) is required. There is concern that the situation will be disadvantageous compared to current light water nuclear power plants. Therefore, future fusion power plants will be required to have extremely high economic efficiency and commercial safety, and in order to obtain high economic efficiency, extremely high-efficiency power generation technology is required for the power generation system connected to the fusion reactor.

In recent years, discussions on supercritical CO_2 gas turbine power generation technology have become active in various countries around the world as a measure to address energy and environmental problems [1-12].

The authors [13-17] are advancing the research and system for practical application of the 3GW$_{th}$ class Free Force Helical Reactor (FFHR) plant model based on the high-efficiency bypass control supercritical CO_2 power generation system and its practical application. It has been clearly shown that it has various advantages such as (1) Engineering design feasibility with a thermal efficiency of 45% or more[13], (2) Minimum compaction of the entire power generation system and low construction cost due to vertical placement, (3) High economic efficiency due to high efficiency, (4) Ease of maintenance due to compact single-axis design of power generation equipment, (5) Easy production with conventional manufacturing technology and materials, (6) High adaptability as commercial heat power source, and (7) Inert, non-toxic cooling medium CO_2 for high plant safety, compared to the case where the system is connected to conventional steam power generation system.

From the viewpoint of the economics of a nuclear fusion reactor where the construction cost of the fusion power plant with high safety is enormous, the design viewpoints from (1) to (7) above are important, such as shortening the depreciation period and improving the power generation efficiency.

In this paper, 3GW$_{th}$-class FFHR power plant model with a molten salt loop for extracting nuclear heat and tritium from the fusion core in the primary system, and a compact and high-efficiency supercritical CO_2 compact gas turbine power generation system for the secondary system was assumed and the optimization of this power generation system by aerodynamic design and the start-up and operation scenario of this power plant model were studied.

Therefore, in Section 2, an overview of the required electric power / thermal energy of each 3GW$_{th}$FFHR component equipment from start-up to operation is given. In Section 3, a basic design was made to determine the specifications and performance of the optimized supercritical CO_2 gas turbine power generation system, and in Section 4, the 3GW$_{th}$FFHR operation scenario with the supercritical CO_2 gas turbine power generation system was examined.

2. Outline of 3GW$_{th}$FFHR power plant model

Minimization of the external heating power to access self-ignition is advantageous to increase the reactor design flexibility and to reduce the capital and operating costs of the plasma heating device in a helical reactor. Recently, O. Mitarai and et.al. reported [18] that a larger density limit leads to a smaller value of the required confinement enhancement factor, a lower density limit margin reduces the external heating power and over 300s of the fusion power rise-up time makes it possible to reach a minimized heating power.

Therefore, here we examined the breakdown of the required heat and electric power required for start-up and operation, and the form of supply, using a helical reactor 3GW$_{th}$ class FFHR power plant model.

2.1 3GWt$_h$FFHR reactor plant model and breakdown of power requirements

Figure 1 shows the 3GW$_{th}$FFHR power plant model [15-17]. Here, the primary system of FLiNaBe for extracting 3GW$_{th}$ heat output and manufactured tritium from the reactor through the blanket from the helical reactor body, and the secondary system of the supercritical CO_2 gas turbine power generation system are connected via an intermediate heat exchanger (IHX)[15].

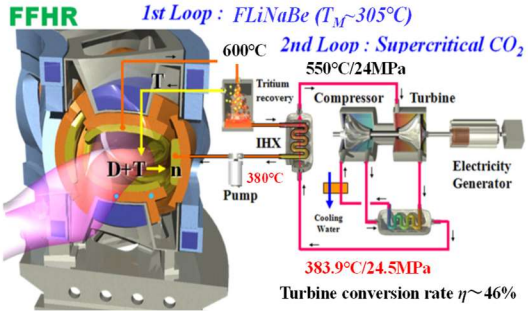

Fig.1 Concept of 3GW$_{th}$FFHR power plant model [17]

2.1.1 Required power during start-up and operation of 3GW$_{th}$FFHR reactor model

This section gives an overview of the required power and thermal energy of each component equipment required for 3GW$_{th}$FFHR start-up and operation. Also, scenarios including supercritical CO_2 gas turbine system will be described in section 4 below. In this section, specific procedures for start-up, operating and stopping each component in the 3GW$_{th}$FFHR power generation facility are summarized as operating scenarios in (i) to (vi).

Figure 2 shows the breakdown of the required heat and electric power required for start-up and operating the 3GW$_{th}$FFHR helical reactor [17-18].

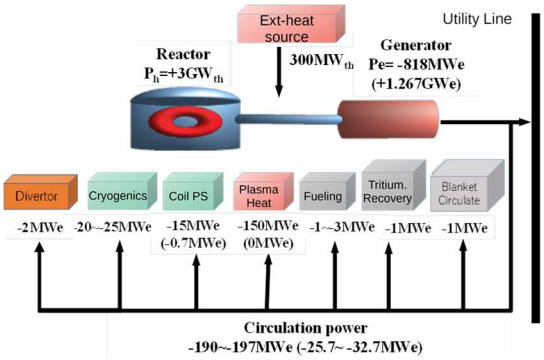

Fig.2 Breakdown of required heat / power during start-up operation of helical reactor in 3GW$_{th}$FFHR power plant model. The required power value when shifting to the steady operation mode is shown in parentheses.[19]

The main required power is supplied to seven systems: a superconducting system (cooling and coil energization), a fuel supply system, a temporary plasma heating system, divertor system for exhaust and cooling(-2MWe), tritium separation and recovery, liquid blanket circulation and purification(-1MWe) and Cryogenic. Of these, the power required for plasma generation to the combustion of the helical reactor body is to supply power to these systems: a superconducting system, a fuel supply system, and a temporary plasma heating system. Furthermore, external power/heat source for driving the primary system of FLiNaBe blanket for 3GW$_{th}$ heat during combustion and production tritium extraction is also requested. Here, the power requirements at start-up from each system are 20~25MWe for cooling in the superconducting system, 15MWe (0.7MWe) for coil energization (Coil PS), 1~3MWe for the fuel system, and 150MWe (0MWe) for temporary plasma heating. Here, the numbers in parentheses are the values during steady operation and the maximum power Coil PS when starting the coil power supply is calculated assuming that the magnetic energy of 170GJ of the superconducting coil is started up in about 8 hours with 80% power supply efficiency (=170GJ/(8h × 3600s) × 2/0.8). The numerator coefficient 2 is a coefficient for obtaining the maximum value when the current is linearly changed at a constant rate. However, the required power value when shifting to the steady operation mode is shown in parentheses. The required external power/heat of the FLiNaBe blanket primary system (includes liquid blanket circulation and purification,1MWe) is approximately 300MW$_{th}$, of which 150MW$_{th}$ is used for FLiNaBe heating and melting, and the rest is used for system heat loss compensation.

The external supply of heat and power necessary for the start-up of the helical reactor will be carried out using the 818MWe(=196MWe(Helical reactor) + 621MWe (CO_2 turbine + 1MWe(Blanket circulation)) class commercial thermal power generation facility and the

400 ° C class exhaust heat from the facility, and all is supplied from the $3GW_{th}$ plasma heat source during operation.

2.1.2 A electric power/heat supply procedure to each component until FFHR start-up

Figure 3 shows a procedure of electric power/heat supply to the helical reactor.

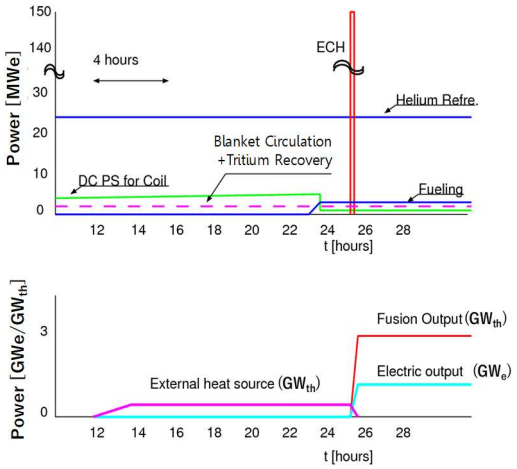

Fig.3 A electric power/heat supply procedure until start-up operation of $3GW_{th}$FFHR power plant model.[19]

In the initial stage of operation, cooling of the superconducting system is started for a long time of about one month, and after that external power/heat and fuel are supplied to the primary system, self-ignition conditions are reached by temporary plasma heating. After that, it shifts to $3GW_{th}$ heat output steady operation, where is not needed plasm current drive as requested in tokamak system.

2.1.3 Optimal design method and design procedure for supercritical CO_2 gas turbine

For the purpose of developing a supercritical CO_2 gas turbine system with a power generation efficiency of 45% or more, the following (1) heat and mass balance analysis for setting the operating conditions of each component, and then (2) The basic design of various components under the these operation conditions was performed.

(1) Heat & mass balance analysis

Based on the initial operating condition values of each power generation system component, heat mass searches for parametric search of various operating conditions of each component (various compressors, turbines, various heat exchangers, etc.) to achieve the highest performance as a power generation system. The purpose is to obtain the optimum solution of power generation performance by performing balance analysis. In this analysis, the power generation efficiency mainly affects the heat adiabatic efficiency of each component, and the efficiency of the power generation system is determined as the sum of the heat adiabatic efficiency of each component.

(2) Basic design of each component

As a result of this heat mass balance analysis, the basic design of each component is performed based on the optimized operating conditions of each component.

In this paper, the heat adiabatic efficiency is raised to the most important design target value during this basic design work, and the specifications of each component device are determined in order to achieve the heat adiabatic efficiency of each component device set in the above heat mass balance analysis.

For example, in the case of a gas turbine, consistency with the set heat adiabatic efficiency is ensured by optimizing the flow rate, inlet temperature, number of stages of rotating rotors, and rotation speed.

In the basic design, the feasibility of the engineering design for each component of the supercritical CO_2 gas turbine designed at the same time is verified.

Finally, the heat mass balance analysis is recalculated based on the heat adiabatic efficiency re-evaluated based on the specifications of each component finally set by the basic design, and the power generation efficiency of the final power generation system is re-evaluated.

The basic specifications of the various constituent components, for example in compressors design, included the dimensions of each part such as the casing diameter, the number of rotary blade stages, and the boss ratio, blade height, cord length, distance between blades, and number of blades in each stage. , degree of reaction, axial flow speed, circumferential speed, pitch code, number of stages, total drag coefficient, dimensionless pressure loss, heat adiabatic efficiency, temperature, pressure, stress induced at blade.

3.Results

3.1 Heat & mass balance of $3GW_{th}$ class Supercritical CO_2 gas turbine power generation system

Here, first assuming that the heat input to the of a $3GW_{th}$-class axial-flow single-shaft control supercritical CO_2 gas turbine power generation system is $3GW_{th}$, the initial values of the following various component operating conditions are given, and heat and mass balance analysis is and an optimization search are performed to obtain maximizing power generation efficiency by searching for various operating parameters based on past conceptual studies under various design conditions shown in Table 1[13].

- Turbine pressure ratio
- Low pressure compressor pressure ratio
- Reactor outlet temperature
- Low and high compressor inlet temperature

- Reactor outlet pressure
- Reactor pressure loss rate
- High pressure side pressure loss of regenerated heat exchangers 1 and 2
- Pressure loss rate on the low pressure side of regenerated heat exchangers 1 and 2
- Pressure loss rate of the front cooler
- Pressure loss rate of the intercooler
- Turbine adiabatic efficiency
- Adiabatic efficiency of low-pressure and high-pressure compressors
- Adiabatic efficiency of bypass compressor
- Average temperature efficiency of regenerated heat exchangers 1 and 2

Table 1 shows the final values of the operating performance conditions re-evaluated from the basic design results described later after performing heat and mass balance analysis based on the above assumed initial values (values in parentheses)

Table 1 Temporary setting value and optimal design conditions of secondary supercritical CO_2 gas turbine power generation system.

Turbine pressure ratio	**2.8**
Low pressure compressor pressure ratio	**1.35**
IHX outlet temperature (℃)	**550**
Compressor inlet temperature (℃)	**35**
IHX outlet pressure (MPa)	**24**
System pressure drop ratio(%)	
IHX	**2**
RHX1(HP)/(LP)	**0.4/1.2**
RHX2(HP)/(LP)	**0.4/1.2**
Precooler	**1**
Intercooler	**0.8**
Compressor adiabatic efficiency(%)	
LPC/HPC/ByC	**83.8/85.6/87.4(88/88/88)**
Turbine adiabatic efficiency(%)	**94.0(92)**
Temperature effectiveness(%)	
RHX 1&2	**91**

※ The numbers in parentheses in the table are temporal values.

In the table, RHX and IHX mean a regenerative heat exchanger (recuperator) and an intermediate heat exchanger, respectively, and HP and LP in the RHX respectively indicate a high pressure side or a low pressure side.

As a result of the heat mass balance analysis of the $3GW_{th}$ class supercritical CO_2 gas turbine power generation system for $3GW_{th}$ heat input, the electric output 1,369MWe can be generated at the supercritical CO_2 flow rate of 12,988kg / s. Therefore, the NET power generation efficiency in this temporary setting value analysis case was estimated to be 45.63%. The power generation efficiency may be further improved by optimizing power generation components described later.

3.2 Basic design of supercritical CO_2 gas turbine power generation components [13]

Here, based on the operating condition values of the various components obtained in (3.1) above, the basic specifications of the various components and the achievable performance were re-evaluated. In re-evaluation, the basic specifications and performance evaluation of rotating equipment such as compressors are the most important.

Therefore, here, the aerodynamic design of various constituent rotating equipment is performed, and the performance dependence on the supercritical CO_2 flow rate, inlet temperature, blade stage number, and rotation speed with respect to the heat adiabatic efficiency target value (indicated by the broken line in the figure) assumed in (3.1) above is determined. The results of the investigation are shown below.

Finally, based on the above results, a uniaxial design structure that combines various compressors and gas turbines to make the power generation system compact, and the relationship between the maximum thermoelectric power generation capacity and the operating rotation speed of various rotating bodies with a common rotation speed. By showing, the maximum power generation capacity of the supercritical CO_2 gas turbine power generation system and the total number of the power generation systems were determined.

3.2.1 Basic aerodynamic design of components

(1) LPC

Figures 4(a) to (d) show the relationship between LPC supercritical CO_2 flow rate, inlet temperature, compressor stage number, control rotation speed, and LPC adiabatic efficiency in a 0.1 to 3GW class supercritical CO_2 gas turbine power generation system. In the figure, the design target values in Table 1 are indicated by broken lines. According to this, However, it was found that a solution satisfying the design target value can be obtained in the verification range for other design items.

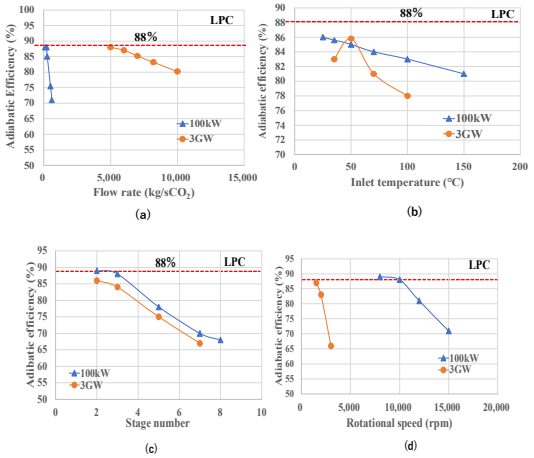

Fig.4 Aerodynamic performance evaluation of Low Pressure Compressor (LPC) in supercritical CO_2 gas turbine power generation system: Relationship between LPC adiabatic efficiency and (a) CO_2 flow rate (b) inlet temperature (c) number of stage stages and (d) rotational speed : In the case of LPC, the adiabatic efficiency that satisfies the uniaxial design point described later in the 3GWth design is 85% or less, and the number of stages at that time needs to be two or more.

(2) HPC

The performance evaluation results related to HPC are shown in Figs.5(a) to (d). As a result, it can be seen that the adiabatic efficiency of the high-pressure compressor has a maximum peak of 88% with respect to the inlet temperature.

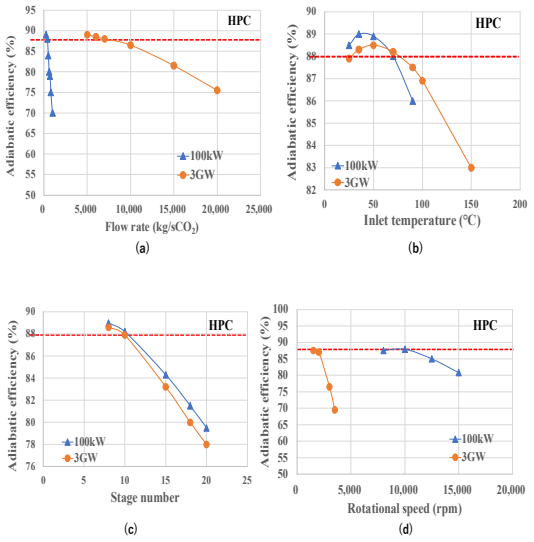

Fig.5 Aerodynamic performance evaluation of High Pressure Compressor (HPC) in supercritical CO_2 gas turbine power generation system: Relationship between LPC adiabatic efficiency and (a) CO_2 flow rate (b) inlet temperature (c) number of stage stages and (d) rotational speed: In the case of HPC, unlike the case of LPC, it can be seen that there are cases where the uniaxial design point can be met at the adiabatic efficiency design target value of 88%.

(3) ByC

The performance evaluation results regarding ByC are shown in Figs.6(a) to (d) as in the above LPC. As a result, although the design target value could not be satisfied in the number of compressor stages, From these results, it is found that there is an optimal solution for the adiabatic efficiency of the bypass compressor in CO_2 flow rate, inlet temperature, number of stages and rotation speed.

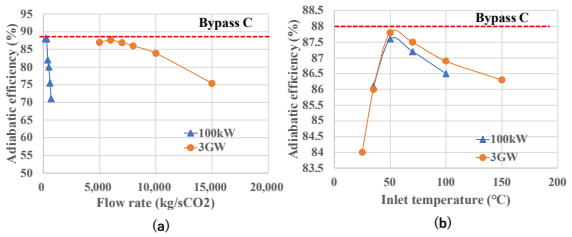

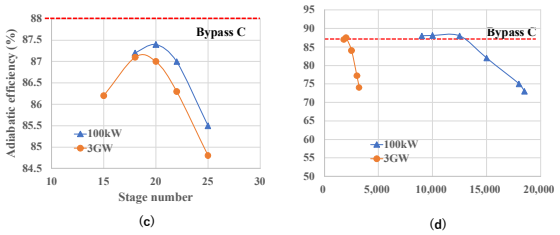

Fig.6 Aerodynamic performance evaluation of Bypass pressure Compressor (ByC) in supercritical CO_2 gas turbine power generation system: Relationship between LPC adiabatic efficiency and (a) CO_2 flow rate (b) inlet temperature (c) number of stage stages and (d) rotational speed: In the case of ByPC, it can be seen that there are cases where the uniaxial design point can be met at the heat adiabatic efficiency design target value of 88%, similar to HPC.

(4) Turbine

Figures 7(a) to (d) show the relationship between turbine performance and adiabatic efficiency of turbine. According to this, unlike the compressor, performance exceeding the design target value can be exhibited depending on the setting conditions.

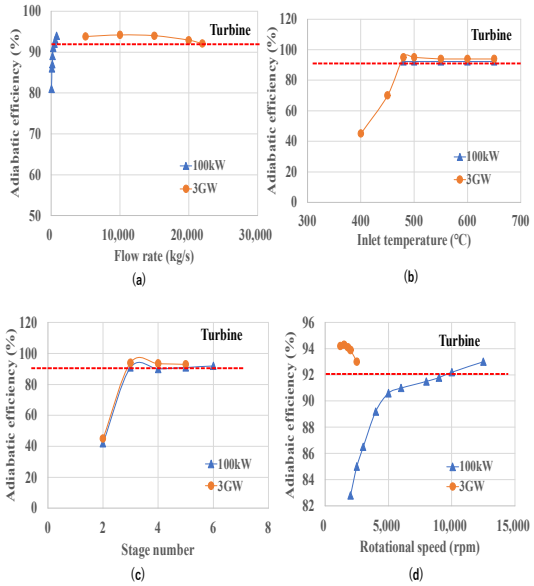

Fig.7 Aerodynamic performance evaluation of Turbine supercritical CO_2 gas turbine power generation system: Relationship between LPC adiabatic efficiency and (a) CO_2 flow rate (b) inlet temperature (c) number of stage stages and (d) rotational speed: In the case of a turbine with $3GW_{th}$ specifications, it can be seen that a high value of 94% adiabatic efficiency can be set at the uniaxial design point.

The optimum design goal of the supercritical CO_2 gas turbine power generation system in this section is to build a system that can maximize the characteristics (1) and (2) in Introduction.

Regarding the compact characteristics of the generation system, the single-shaft design in which the various compressors, turbine, and generator shown in the conceptual diagram of Fig.13 below are connected via a single shaft is the best way to make this power generation system compactness.

Therefore, here, we searched for conditions that maximize the power generation efficiency from 3GW$_{th}$FFHR by matching the design conditions that enable this uniaxial design with the performance conditions.

3.2.2 Design limit range and single shaft design

In the above section (3.2.1), the aerodynamic and mechanical properties within the various parameter ranges such as CO_2 flow rate, inlet temperature, number of stages, etc. under specific adiabatic efficiency in various compressors and gas turbines.

Table 2 shows the allowable design limits for each component derived in the typical model cases of 100MW$_{th}$ and 3GW$_{th}$ heat source from these results.

Here, from the design limit ranges of various component devices, a component device structure that satisfies all the requirements (1) to (7) of the Induction 1. was studied and selected.

Table 2 The allowable design limits for each component derived in the typical model cases of 100MW$_{th}$ and 3GW$_{th}$ heat input: The numbers in parentheses in the table are the values of 3GW$_{th}$ heat input.

Component	LHP	HPC	ByC	Turbine
Allowable CO_2 flow rate range(kg/s)	50~400 (7,000~10,000)※	250~600 (5,000~10,000)※	200~500 (5,000~13,000)※	200~800 (5,000~22,000)※
Allowable inlet temperature range(℃)	25~150 (25~100)※	25~95 (35~200)※	35~90 (25~150)※	500~650
Allowable step number range(step)	1~4 (2~3)※	8~20 (6~18)※	18~25 (15~25)※	3~6 (3~5)※
Allowable speed range(rpm)	8,000~12,000 (1,500~2,000)※	8,000~15,000 (1,500~3,500)※	8,000~15,000 (1,800~3,200)※	8,000~13,000 (1,000~2,500)※

※The numbers in parentheses in the table are the values of 3GW$_{th}$ heat input.

Fig. 8 shows a minimum design case in which the requirement (2) in chapter 1. is emphasized. Here, the minimum axial length and the minimum diameter of various compressors and turbines which are satisfied within the design limit range given in table 4 and various structural equipment structural design are shown. As a result of the physique design and performance evaluation of these major components, it was found that both were within the design tolerance and had a shape and performance that could be manufactured and used.

Fig. 8 also shows the total structure design for a single shaft of 0.1 GW$_{th}$ and 1.5 GW$_{th}$ (×2). The total length of two 1.5GW$_{th}$ class supercritical CO_2 gas turbine power generation systems connected to 3GWthFFHR is about 5m (excluding power generators) each, and is designed to be extremely compact compared to conventional steam power generation turbo equipment.

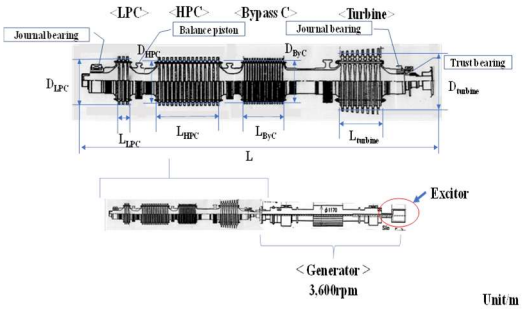

Unit/m

Power	L_{LPC}	L_{HPC}	L_{ByC}	$L_{turbine}$	D_{LPC}	L	D_{HPC}	D_{ByC}	$D_{turbine}$
0.1GW	0.16	0.34	0.98	0.22	0.16	2.5	0.14	0.18	0.3
1.5GW	0.28	0.89	2.5	0.44	0.45	5.0	0.39	0.5	0.75

Fig. 8 Layout of 0.1~1.5GW$_{th}$ class supercritical CO_2 gas turbine power generation system

3.2.3 Power generation speed and power generation scale synchronized by uniaxial design

Optimal uniaxial design is possible because the rotation speed at the highest performance that can be achieved by each component rotating device is the same for all component devices.

From the relationship between the rotation speed and heat adiabatic efficiency during operation of various compressors and turbines obtained in (3.2) above, it is possible to know the relationship between the common rotation speed of these constituent rotating devices and the power generation scale at that rotation speed.

Fig.9 shows the relationship of the control rotational speed with respect to the heat input of 0.1 to 3GW$_{th}$ of supercritical CO_2 gas turbine power generation system

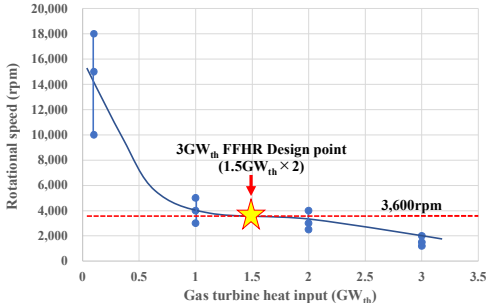

Fig.9 Relationship between heat input and control speed of supercritical CO_2 gas turbine power generation system

As a result, it can be seen that the rotational speed decreases as the heat source input increases. In the figure, the required rotation speed of the power generation system in the shared frequency band (50~60Hz) for power supply in Japan is shown with a star symbol.

When designed at a high speed for this set speed band (up to 3,600 rpm), the power generation system requires

a speed reducing mechanism, and when designed at a low speed, a speed increasing mechanism or frequency conversion is required. Therefore, in any case, it is difficult to make the power generation system compact.

However, in the case of 3GW$_{th}$FFHR, there is a set rotation speed band just at the heat input of 1.5GW$_{th}$, so by connecting two (= 1.5GW$_{th}$ x 2) supercritical CO_2 gas turbine power generation systems to FFHR, the power generation system alone can be made more compact, and it is possible to improve cost performance by constructing a power generation system of the same scale with a minimum of two.

Table 3 shows the results of re-evaluating the power generation efficiency of the power generation system using the high performance turbine values selected from the design limit range described in section 3.2.2 as the turbine performance that can be synchronized with the rotational speed in Fig.9. As a result, the power generation efficiency improved by about 1% (46.91%=1,267MWe/2,700MW$_{th}$) from the temporary setting value forecast (45.63%).

Table 3 Comparison of temporary setting value and optimal design conditions and performances of 1.5GW$_{th}$ supercritical CO_2 gas turbine power generation system components.

	η_{LPC}	η_{HPC}	η_{ByC}	$\eta_{turbine}$	η_{system}
Stage number	1	6	13	4	——
Temporal data	88.0	88.0	88.0	92.0	45.63
Optimal data	88.1	86.7	87.9	94.0	46.91

3.2.4 Components design and its performance

Here, the basic design specifications for compressors and turbines and their predicted performance are mainly shown. We also verified engineering feasibility the performance of the designed compressors and turbines during operation.

(1) Components design and its performance

Figure 10 shows the casing diameters and blade heights of various compressors and turbines of the 1.5GW$_{th}$ supercritical CO_2 gas turbine designed in the previous section.

The casing diameter decreases as the stage increases, and the bypass compressor becomes the maximum size, followed by the low-pressure compressor and then the high-pressure compressor. The casing diameter of the gas turbine decreases sharply as the stage increases. Regarding the blade height, the one with the high-pressure compressor was the largest, followed by the bypass compressor and the low-pressure compressor.

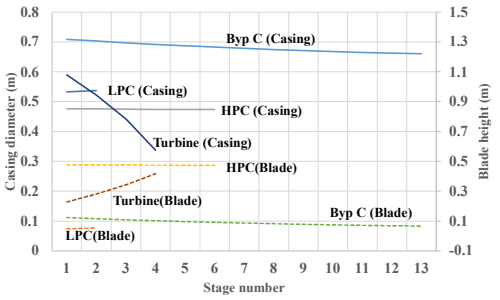

Fig.10 The casing diameters and blade heights of various compressors and turbines of the 1.5GW$_{th}$ supercritical CO_2 gas turbine.

Contrary to the compressor, the height of the compressor blade increased as the stage became higher, and the height became an intermediate size between the high-pressure compressor and the bypass compressor.

Figure11 shows the changes in total pressure and temperature at each stage of the 1.5GW$_{th}$ supercritical CO_2 gas turbine. Among the various compressors, the compressor with the largest pressure change is the high-pressure compressor, followed by the bypass compressor. The temperature rise during compression was highest in the bypass compressor, and decreased in the order of the low-pressure compressor and the high-pressure compressor.

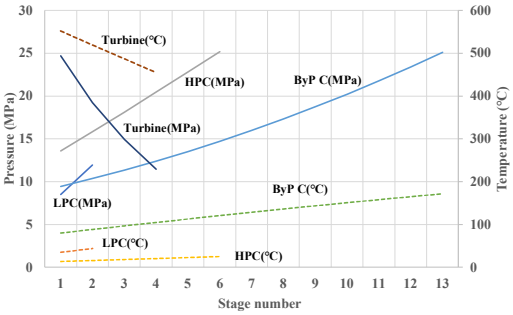

Fig.11 The changes in total pressure and temperature at each stage of the 1.5GW$_{th}$ supercritical CO_2 gas turbine.

(2) Verification of engineering feasibility

Here, in order to verify the design feasibility of the 1.5 GW$_{th}$ supercritical CO_2 gas turbine designed in the previous chapter, the fluid characteristics generated in each stage of various compressors and turbine and the margin of generated stress with respect to the allowable stress were verified.

Figure 12 shows the de Haller number [22] and the diffusion factor [23] in each compressor and each stage of the 1.54GW$_{th}$ supercritical CO_2 gas turbine. The former is a condition for preventing peeling of the boundary layer along the wall in an axial compressor, and is recommended to be 0.7 or more. According to this value, it can be seen that this condition is cleared in various compressors.

On the other hand, the diffusion coefficient in the case of a compressible fluid is recommended to be 0.5 or less, and it can be seen that this condition is satisfied in all the designed components.

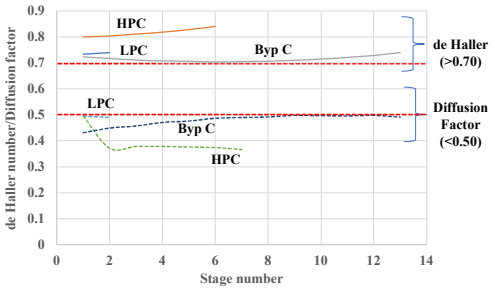

Fig.12 The de Haller number[22] and the diffusion factor[23] in each compressor and stage of the 1.5GW$_{th}$ supercritical CO_2 gas turbine.

Figure 13 shows the Reynolds number[24] and blade stress at each stage during operation of the 1.5GW$_{th}$ supercritical CO_2 gas turbine. Operating a compressor at a low Reynolds number increases friction loss and affects the efficiency of the power generation system, so a value of 2.5×10^5 or higher is recommended.

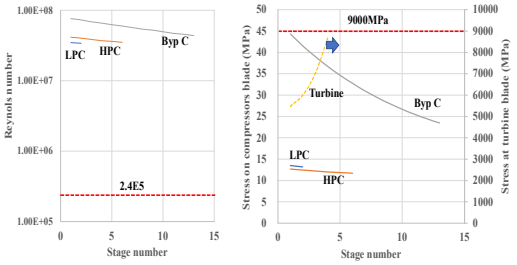

Fig.13 The Reynolds number[24] and blade stress at each stage during operation of the 1.5GW$_{th}$ supercritical CO_2 gas turbine.

As a result of the analysis, the values are 1.0×10^7 or more in all the constituent devices, and it can be seen that the influence of friction loss is small in this design.

The combined stress due to the centrifugal force and gas bending force applied to the moving blade during operation is the highest in turbine power, and it is essential to use a high-temperature/high-strength material (> 9000 MPa) made of unidirectional solidified crystals. On the other hand, the stress generated by the compressor power is 50MPa or less, and the material problem can be avoided.

4. 3GW$_{th}$FFHR start-up/operation scenario

Figure 14 shows the conceptual diagram of the FLiNaBe primary system and the secondary system of the supercritical CO_2 gas turbine power generation system connected to 3GW$_{th}$FFHR, and the heat mass balance during steady operation. The electrothermal conversion efficiency of the 3GW$_{th}$FFHR power plant connected with the optimally designed supercritical CO_2 gas turbine power generation system was estimated to be 40.65%(=1,219.45MWe/3,000MW$_{th}$).

For simplicity, it is assumed that there is one secondary supercritical CO_2 gas turbine power generation system, and the 3GW$_{th}$FFHR start-up / run / stop scenario was examined. The heat input through the IHX to the supercritical CO_2 gas turbine power generation system is 2.7 GW$_{th}$ (= 3-0.3 (GW$_{th}$)) in consideration of the IHX heat exchange efficiency (90%).

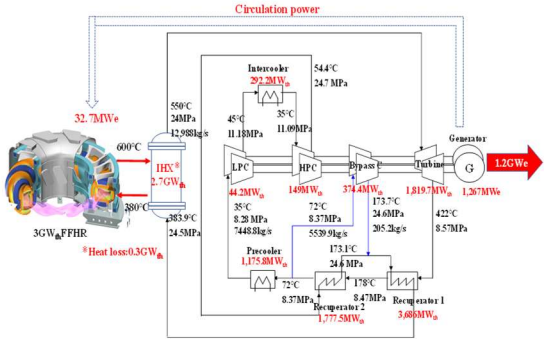

Fig.14 Optimally designed 3GW$_{th}$FFHR power plant model(1.5GW$_{th}$ super critical CO_2 gas turbine$\times$2) and its heat mass balance.

Table 4 shows a summary and breakdown of the power/heat required for each component system of the helical reactor and the primary and secondary systems from start-up, self-ignition to self-sustained operation. The numbers in parentheses in the table are the values during steady operation. Regarding the required energy for plasma stability and combustion control, while the tokamak reactor requires additional steady-state energy input for plasma current drive, etc., the helical reactor without the threat of plasma disruption does not require it.

Table 4 Breakdown of required power during start-up of each component of optimal 3GW$_{th}$FFHR power plant model: The numbers in parentheses in the table are the values during steady operation.

Equipment's	*Demand MWe/MW$_{th}$*		
FLiNaBe primary system			
Liquid blanket circulation and purification	-1	-1MWe	
Coolant melting heat source	-150(0)※	300MW$_{th}$(0)※	
Heat loss compensation	-150(0)※		
Super critical CO_2 secondary system			
LPC	-44	-621MWe (+1,267MWe)※	-818MWe (+1,234MWe)※
HPC	-166		
ByC	-411		
Turbine	-0.1(+1,886)※		
Helical reactor (3GW$_{th}$)※			
Cryogenic	-20~-25	-196MWe (-31.7MWe)※	
Coil SP	-15(-0.7)※		
Plasma heat	-150(0)※		
Fueling	-1~-3		
Divertor system for exhaust and cooling	-2		
Tritium recovery	-1		

※The numbers in parentheses in the table are the values during steady operation.

The external commercial power source here is premised on an electric power supply and heat environment that can be supplied from an existing facility (818MWe class thermal power generation plant) at any time by an external electric power network other than the reactor.

The scenario of starting a nuclear fusion power plant is assumed because the background of the social energy supply structure differs between the first generation type(Generation I) in the latter half of the 21st century and the second generation type after that(Generation II).

It is most realistic and economical that the start-up / operation scenario of the first generation $3GW_{th}$FFHR in Generation I is exclusively performed by cogeneration from the existing 818MWe class thermal power plant. At the same time as the construction of the first $3GW_{th}$FFHR, 818MWe backup thermal power plant (power generation efficiency of about 40%) will be constructed nearby, and 818MWe power supply and $300MW_{th}$ waste heat at about 400 ° C will be supplied together to start-up the $3GW_{th}$FFHR power plant.

However, in a power system that is not robust to short-term power fluctuations, such as Japan's elongated power grid, receiving large amounts of temporarily fluctuating power directly from the grid when starting up a power plant woace a stress on the other power plants connected tould pl the grid and the grid control system, and would cause disturbance to the entire grid. In order to avoid this, a system in which an external source is prepared and the energy required at startup is supplied from outside the power grid in Generation I.

Although this external source will have to be adjusted to match the increased power of the fusion plant itself, it will be able to limit the upset of the entire power system.

Consequently, the transformers and high-voltage switches required to connect and disconnect external sources are on the same scale as those installed at large thermal and nuclear power plants in the 500MWe to 1GWe class that are currently installed in the power system, and are already well established.

The connection and disconnection procedures for external sources and fusion reactors are also assumed to be similar to those for the connection and disconnection of existing large thermal power plants to the power grid.

In Generation II, since multiple $3GW_{th}$-class FFHR power plants have already been built, 818MWe and $300MW_{th}$ worth of electric power required for starting up a new power plant will be provided entirely by electric power from other FFHR power plants via the electric power supply network.

(i) Start-up of Helical reactor [20]

The power supply of up to 25MWe will be supplied from an external commercial power source and cooling of the superconducting cryostat of the helical furnace will be started over approximately 30 days. Next, An electric power of 15MWe is supplied as power for starting the ECH device for plasma generation. At this time, it is assumed that the following FLiNaBe primary system and supercritical CO_2 gas turbine power generation system has already been started. Subsequently, plasma heating is started by ECRH, and after heating to the self-ignition state, fuel is injected (1~3MWe) and $3GW_{th}$ operation is started.

(ii) Start-up the FLiNaBe primary system

The power supply of up to $300MW_{th}$ is supplied from 400 ℃ class exhaust heat from 818MWe class commercial thermal power plant and the heat release ($150MW_{th}$) from the primary system is compensated and the phase of the molten salt is changed from solid to molten($150MW_{th}$). The primary system circulation pump and purification system of liquid blanket is activated by 1MWe power supply, and the circulation operation of the molten salt in the primary system is started. About 30 days are assumed for the start-up of the FLiNaBe primary system.

(iii) Start-up the supercritical CO_2 gas turbine power system

Slightly delayed from the primary system operation, the heat output from the helical furnace after plasma ignition is transferred to the primary system, and then the operation of the secondary system of the supercritical CO_2 gas turbine power generation system is started.

567.6MWe, which is mainly required for compressor power of the supercritical CO_2 gas turbine power generation system, is supplied from an external commercial power source through an exciter attached to the generator, and the function of the generator is converted to a motor to restore CO_2 in the secondary system.

(iv) Steady operation mode

As the fuel supply starts after plasma ignition, the heat source output in the helical reactor increases, and the electrical output from the secondary system can be obtained by heat transfer to the primary system and secondary system. From this state, the in-house power from the external commercial power is gradually switched to the internal power, and when the maximum output reaches $3GW_{th}$, the external commercial power is replaced with the internal power.

The breakdown of the required power in the station in the steady operation state is the fuel system 1~3MWe, the coil power supply 0.7MWe, the cryostat power supply 20~25MWe and the primary circulation power pump power supply 1MWe. That is, a total of 32.7MWe of power is supplied from the total generated power as the in-house required power.

According to this, the maximum required power/heat of each component system at start-up is $300MW_{th}$ for the primary FLiNaBe system, 568MWe for the secondary system, and 190~197MWe for circulation power, which requires 818MWe/$300MW_{th}$ class power supply / heat at the peak. This required heat / power is comparable to the capacity of multiple thermal power plants.

(v) Utility

In the future, a part of the net generated power (<1%) will be used for hydrogen production at all times and will be stored in the station as start-up fuel. This will be used as internal power/heat source supply when starting the power plant [21].

(vi) Shutdown

The plant is completely shut down by erasing the plasma by gradually shutting off the fuel supply and magnetic field power supply, lowering the heat output and simultaneously moving the primary and secondary cooling media to the reservoir tank.

5. Conclusions

As a result of optimizing the power generation system for the $3GW_{th}$ class FFHR power plant model with the supercritical CO_2 gas turbine power generation system with bypass control, and the operation scenario and power generation performance evaluation of the plant model, the following conclusions were obtained.

(1) The most efficient and compact axial flow uniaxial design supercritical CO_2 gas turbine power generation system suitable for $3GW_{th}$FFHR power plant has a maximum heat capacity of $1.5GW_{th}$ with 5m length including compressors and turbine parts, and the power generation efficiency at that time was evaluated as 46.38%. Therefore, split connection with two power generation systems is optimal for a $3GW_{th}$ class FFHR power plant. Here, the operating speed of the turbo equipment was set to 3,600 rpm in order to adapt this plant model to the power supply system in Japan.

(2) The required peak power/heat at start-up of the power plant model is estimated to be equivalent to a maximum of 818MWe/$300MW_{th}$, and it is necessary to supply and maintain the same electric powers and heat for about 300 sec and 30days each from start-up to the transition to steady operation.

(3) The in-house power during steady operation under the self-ignition condition was reduced to about 32.7MWe, and the amount of power generated at the transmission end was evaluated as 1,219MWe (= $1,219MW_e/3,000MW_{th}$ (40.65%)).

References

[1] C. W. White, N. T. Weiland, W. W. Shelton and T. R. Shultz, The 6th International Supercritical CO_2 Power Cycles Symposium March 27 - 29, 2018, Pittsburgh, Pennsylvania, 135.

[2] M. Penkuhn, G. Tsatsaronis, The 6th International Supercritical CO_2 Power Cycles Symposium March 27 - 29, 2018, Pittsburgh, Pennsylvania, 052.

[3] P.Sharan, T. Craig, T. Neises, The 6th International Supercritical CO_2 Power Cycles Symposium March 27 - 29, 2018, Pittsburgh, Pennsylvania, 187.

[4] J. Cho, H. Shin, H. Ra, C. Roh and et.al., The 6th International Supercritical CO_2 Power Cycles Symposium March 27 - 29, 2018, Pittsburgh, Pennsylvania, 102.

[5] A. Chaudhary, Y. Trivedi, A. Mulchand, H. Chauhan, P. Dave and et.al., The 6th International Supercritical CO_2 Power Cycles Symposium March 27 - 29, 2018, Pittsburgh, Pennsylvania, 051.

[6] C. Spadacini, E. Pesatori, L. Centemeri, N. Lazzarin and et.al., The 6th International Supercritical CO_2 Power Cycles Symposium March 27 - 29, 2018, Pittsburgh, Pennsylvania, 113.

[7] J.Schmitt, J.Nielson and N.Poerner, The 6th International Supercritical CO_2 Power Cycles Symposium March 27 - 29, 2018, Pittsburgh, Pennsylvania, 090.

[8] M. Enoeda, Y. Kosaku, T. Hatano, et. al., 2003. Design and technology development of solid breeder blanket cooled by supercritical water in Japan. J. Nucl. Fusion 43, 1837e1844.

[9] T. Ishizuka, Y. Kato, et al., 2005. Thermal-hydraulic characteristics of printed circuit heat exchanger in super critical CO2 loop. In: Proceedings of NURETH-11, October 2e6, Avignon, France.

[10] Y. Kato, T. Nitawaki, Y. Muto, 2004. Medium temperature carbon dioxide gas turbine reactor. Nucl. Eng. Des. 230, 195e207.

[11] Y. Kato, Y. Muto, T. Ishizuka, M. Mito, 2005. Design of recuperator for the supercritical CO2 gas turbine fast reactor. In: Proceedings of ICAPP05, #5196, May 15e19, Seoul, Korea.

[12] M. Mito, N. Yoshioka, et al., 2006. Fast reactor with indirect cycle system of supercritical CO_2 gas turbine plant. In: Proceedings of ICAPP06, #6265, June 4e8, Reno, NV, USA.

[13] S. ISHIYAMA, Y. Muto, Y. Kato, S. Nishio, T., Hayashi, and Y. Nomoto, Progress in Nuclear Energy Vol.50, No.12-6,325-332(2008)

[14] S. Ishiyama, T. Tanaka, A. Sagara, and H. Chikaraishi, Fusion Science and Technology, DOI: https://doi.org/10.1080/15361055.2019.1658046(2019)

[15] A. Sagara, T. Tanaka,a J. Yagi, M. Takahashi, K. Miura, T. Yokomine, S. Fukada, and S. Ishiyama, FUSION SCIENCE AND TECHNOLOGY VOL. 68, 303-307, SEP. 2015

[16] A. Sagara*, H. Tamura, T. Tanaka, N. Yanagi, J. Miyazawa, T. Goto, R. Sakamoto, J. Yagi, T. Watanabe, S. Takayama, the FFHR design group, Helical reactor design FFHR-d1 and c1 for steady-state DEMO, Fusion Engineering and Design 89 (2014) 2114–2120.

[17] A. Sagara, J. Miyazawa, H. Tamura, T. Tanaka, T. Goto, N. Yanagi, R. Sakamoto, S. Masuzaki, H. Ohtani and The FFHR Design Group, Two conceptual designs of helical fusion reactor FFHRd1A based on ITER technologies and challenging ideas, Nucl. Fusion **57** (2017) 086046 (6pp)

[18] O. Mitarai1, A. Sagara, H. Chikaraishi, S. Imagawa, K.Watanabe, A. A. Shishkin and O. Motojima, Minimization of the external heating power by long fusion power rise-up time for self-ignition access in the helical reactor FFHR2m, Nucl. Fusion **47** (2007) 1411–1417.

[19] NIFS Peer Review Reports in FY2013, P122.

[20] ITER-EDA-DS-22, ITER

EDADOCUMENTATION SERIES NO. 22
International Thermonuclear Experimental Reactor (ITER) Engineering Design Activities (EDA)
SUMMARY of the ITER FINAL DESIGN REPORT
July 2001.
[21] S. Yamada, A. Sagara, S. Imagawa, O. Motojima, Study on hydrogen production from steam electrolysis in LHD-type power reactor FFHR, Fusion Engineering and Design 84 (2009) 1997–2001
[22] P.de Haller, BWK, Bd.5, Ht.10, P.333-337(1953).
[23] S.L. Dixon B. Eng., Ph.D., C.A. Hall Ph.D., in Fluid Mechanics and Thermodynamics of Turbomachinery (Seventh Edition), 2014
[24] Heidelberg, L. J., Ball, C. L, Weigel, C., Effect of Reynolds Number on Overall Performance of A 6 —inch Radial Bladed Centrifugal Compressor. NASA TN D-5761(1970).

Tables and figures

Table 1 Temporary setting value and optimal design conditions of secondary supercritical CO_2 gas turbine power generation system.

Table 2 The allowable design limits for each component derived in the typical model cases of $100MW_{th}$ and $3GW_{th}$ heat input: The numbers in parentheses in the table are the values of $3GW_{th}$ heat input.

Table 3 Comparison of temporary setting value and optimal design conditions and performances of $1.5GW_{th}$ supercritical CO_2 gas turbine power generation system components.

Table 4 Breakdown of required power during start-up of each component of optimal $3GW_{th}$FFHR power plant model.

Figure 1 Concept of $3GW_{th}$FFHR power plant model [16]

Figure 2 Breakdown of required heat / power during start-up operation of $3GW_{th}$FFHR power plant model.[18]

Figure 3 A electric power/heat supply schedule until start-up operation of $3GW_{th}$FFHR power plant model.[18]

Figure 4 Aerodynamic performance evaluation of Low Pressure Compressor (LPC) in supercritical CO_2 gas turbine power generation system: Relationship between LPC adiabatic efficiency and (a) CO_2 flow rate and (b) inlet temperature, (c) number of stage stages, (d) rotational speed

Figure 5 Aerodynamic performance evaluation of High Pressure Compressor (HPC) in supercritical CO_2 gas turbine power generation system: Relationship between LPC adiabatic efficiency and (a) CO_2 flow rate, (b) inlet temperature, (c) number of stage stages, (d) rotational speed

Figure 6 Aerodynamic performance evaluation of Bypass pressure Compressor (ByC) in supercritical CO_2 gas turbine power generation system: Relationship between LPC adiabatic efficiency and (a) CO_2 flow rate, (b) inlet temperature, (c) number of stage stages, (d) rotational speed

Figure 7 Aerodynamic performance evaluation of Turbine in supercritical CO_2 gas turbine power generation system: Relationship between LPC adiabatic efficiency and (a) CO_2 flow rate, (b) inlet temperature, (c) number of stage stages, (d) rotational speed

Figure 8 Layout of 0.1~1.5GW_{th} class supercritical CO_2 gas turbine power generation system

Figure 9 Relationship between heat input and control speed of supercritical CO_2 gas turbine power generation system

Fig.10 The casing diameters and blade heights of various compressors and turbines of the 1.5GW_{th} supercritical CO_2 gas turbine.

Fig.11 The changes in total pressure and temperature at each stage of the 1.5GW_{th} supercritical CO_2 gas turbine.

Fig.12 The de Haller number[22] the diffusion factor [23] of each compressor and stage of the 1.5GW_{th} supercritical CO_2 gas turbine.

Fig.13 The Reynolds number[24] and blade stress in each stage during operation of the 1.5GW_{th} supercritical CO_2 gas turbine.

Fig.14 Optimally designed 3GW_{th}FFHR power plant model(1.5GW_{th} super critical CO_2 gas turbine × 2) and its heat mass balance.